

# FasTer: Fast Tensor Completion with Nonconvex Regularization

Quanming Yao<sup>1</sup> James T. Kwok<sup>2</sup> Bo Han<sup>3</sup> Weiwei Tu<sup>1</sup>

4Paradigm Inc, Beijing, China<sup>1</sup>

Hong Kong University of Science and Technology, Hong Kong<sup>2</sup>

University of Technology Sydney, Sydney, Australia<sup>3</sup>

correspondence to: yaoquanming@4paradigm.com

## Abstract

Due to the easy optimization, the convex overlapping nuclear norm has been popularly used for tensor completion. However, it over-penalizes top singular values and lead to biased estimations. In this paper, we propose to use the nonconvex regularizer, which can less penalize large singular values, instead of the convex one for tensor completion. However, as the new regularizer is nonconvex and overlapped with each other, existing algorithms are either too slow or suffer from the huge memory cost. To address these issues, we develop an efficient algorithm, which is based on the proximal average (PA) algorithm, for real-world problems. Compared with the direct usage of PA algorithm, the proposed algorithm runs orders faster and needs orders less space. We further speed up the proposed algorithm with the acceleration technique, and show the convergence to critical points is still guaranteed. Experimental comparisons of the proposed approach are made with various other tensor completion approaches. Empirical results show that the proposed algorithm is very fast and can produce much better recovery performance.

## 1 Introduction

Tensors, which can be seen as high-order matrices, have been commonly used to describe the multilinear relationships inside the data. In this paper, we focus on 3-order tensors, since they naturally appear in many applications. For example, the color image can be seen as 3-order tensor (Liu et al. 2013); in remote sensing applications, a hyperspectral image with multiple bands can be naturally represented as a 3-order tensor (Signoretto et al. 2011); in Youtube’s social network, users can follow each other and can have the same subscribed channels. By treating these attributes as another dimension, rating prediction becomes a problem on the 3-order tensor (Lei, Wang, and Liu 2009).

However, usually, we can only have a few observations in these tensors. Low-rank tensor completion is popularly used for filling and predicting these unseen values (Tomioka, Hayashi, and Kashima 2010; Acar et al. 2011; Song et al. 2017). Mathematically, let the observed elements indicating by 1’s in the binary tensor  $\Omega \in \{0, 1\}^{I_1 \times I_2 \times I_3}$  with values given by corresponding positions in  $\Theta \in \mathbb{R}^{I_1 \times I_2 \times I_3}$ , the

low-rank tensor completion problem is <sup>1</sup>

$$\min_{\mathcal{X} \in \mathbb{R}^{I_1 \times I_2 \times I_3}} \frac{1}{2} \|P_{\Omega}(\mathcal{X} - \Theta)\|_F^2 + \lambda r(\mathcal{X}), \quad (1)$$

where  $r$  is a regularizer encouraging  $\mathcal{X}$  to be low-rank, and  $[P_{\Omega}(\mathcal{X})]_{i_1 i_2 i_3} = \mathcal{X}_{i_1 i_2 i_3}$  if  $\Omega_{i_1 i_2 i_3} = 1$  and 0 otherwise.

Recently, due to the success of the nuclear norm for low-rank matrix completion (Candès and Recht 2009), convex relaxation of tensor rank based on the nuclear norm are also introduced for tensor completion (Tomioka, Hayashi, and Kashima 2010; Gandy, Recht, and Yamada 2011). Common examples of  $r$  include the tensor trace norm (Chandrasekaran et al. 2012), overlapped nuclear norm (Tomioka, Hayashi, and Kashima 2010; Gandy, Recht, and Yamada 2011), and latent nuclear norm (Tomioka, Hayashi, and Kashima 2010). Among them, the overlapped nuclear norm is the most popular ones. Compared with the tensor trace norm, it can be computed exactly without the approximation (Cheng et al. 2016). Then, it can encourage tensor to be low-rank on every mode simultaneously, which can better approximate a low-rank tensor than the latent nuclear norm (Tomioka, Hayashi, and Kashima 2010). Besides, the theoretical guarantee has also been provided, which shows the exact recovery is possible (Tomioka et al. 2011; Tomioka and Suzuki 2013; Mu et al. 2014).

However, one potential problem of the nuclear norm is that it equally penalizes all singular values, while the larger singular values can be more informative (Mazumder, Hastie, and Tibshirani 2010). To less penalize large singular values, adaptive nonconvex regularizers, have been introduced for low-rank matrix learning. Examples are, capped- $\ell_1$  norm (Zhang 2010b), log-sum-penalty (LSP) (Candès, Wakin, and Boyd 2008), truncated nuclear norm (TNN) (Hu et al. 2013), smoothed-capped-absolute-deviation (SCAD) (Fan and Li 2001) and minimax concave penalty (MCP) (Zhang 2010a). They give both better empirical performance (Lu et al. 2016; Yao et al. 2018) and statistical guarantee (Gui, Han, and Gu 2016) than the convex nuclear norm. Besides, these regularizers have not been used for tensor completion yet.

Motivating by the problem of over-penalizing top singular values of the convex nuclear norm, we propose to use nonconvex penalties with overlapped nuclear norm as  $r$  in

<sup>1</sup>Without loss of generality, we assume that  $I_1 \geq I_2 \geq I_3$ .

(1). Since the regularizers are nonconvex and overlap with each other, the resulting problem is hard to optimize. We first find that the proximal average (PA) algorithm (Zhong and Kwok 2014) becomes the only applicable algorithm which also has the convergence guarantee.

Unfortunately, due to the needs of folding and unfolding operations of tensor, PA algorithm suffers from the extremely large space requirement and expensive iteration complexity. These greatly limit the usage of the new model in real problems, especially when the data scale is large. To address these issues, we propose an important proposition avoiding such operations in iterations of PA algorithm. Moreover, we adopt the acceleration technique to speed up the convergence of PA algorithm, while still offers the convergence guarantee. This helps to significantly cut down the number of iterations required by PA algorithm. As a result, the proposed algorithm needs orders less memory but runs orders faster than the direct usage of PA algorithm. Finally, we perform experiments on both synthetic and real data sets. Results show that the proposed algorithm is very efficient and can produce much better empirical performance than other tensor regularization and decomposition methods.

**Notation** In the sequel, vectors are denoted by lowercase boldface, matrices by uppercase boldface, and tensors by boldface Euler. For a matrix  $\mathbf{A}$  with singular values  $\sigma_i$ 's, its nuclear norm is  $\|\mathbf{A}\|_* = \sum_i \sigma_i$ . We follow the tensor notation in (Kolda and Bader 2009). For a 3-order tensor  $\mathcal{X} \in \mathbb{R}^{I_1 \times I_2 \times I_3}$ , its  $(i_1, i_2, i_3)$ th entry is  $\mathcal{X}_{i_1 i_2 i_3}$ . We can *unfold*  $\mathcal{X}$  along its  $d$ th-mode to obtain the matrix  $\mathbf{X}^{(d)} \in \mathbb{R}^{I_d \times (I_1 \times I_2)}$ , with elements  $\mathbf{X}_{i_1 i_2 j}^{(d)} = \mathcal{X}_{i_1 i_2 i_3}$ , where  $j = 1 + \sum_{l=1, l \neq d}^3 (i_l - 1) \prod_{m=1, m \neq d}^{l-1} I_m$ . We can also *fold*  $\mathbf{X}$  back to a tensor, i.e.,  $\mathcal{X} = \mathbf{X}^{(d)}$ , with elements  $\mathcal{X}_{i_1 i_2 i_3} = \mathbf{X}_{i_1 i_2 j}^{(d)}$ , where  $j$  is as defined above. The inner product of two tensors  $\mathcal{X}$  and  $\mathcal{Y}$  is  $\langle \mathcal{X}, \mathcal{Y} \rangle = \sum_{i_1=1}^{I_1} \sum_{i_2=1}^{I_2} \sum_{i_3=1}^{I_3} \mathcal{X}_{i_1 i_2 i_3} \mathcal{Y}_{i_1 i_2 i_3}$ , and the Frobenius norm of  $\mathcal{X}$  is  $\|\mathcal{X}\|_F = \sqrt{\langle \mathcal{X}, \mathcal{X} \rangle}$ .

## 2 Related Works

### 2.1 Nonconvex Low-Rank Matrix Regularization

Nonconvex regularizers, such as the capped- $\ell_1$  norm, LSP and TNN, have been introduced in low-rank matrix learning. They can less penalize the larger, more informative singular values. Thus, they also have better empirical performance and theoretical guarantee than nuclear norm regularization (Lu et al. 2016; Gui, Han, and Gu 2016; Yao et al. 2018). The optimization problem is formulated as

$$\min_{\mathbf{X} \in \mathbb{R}^{I_1 \times I_2}} f(\mathbf{X}) + \lambda \phi(\mathbf{X}), \quad (2)$$

where  $f$  is a  $\rho$ -Lipschitz smooth loss, (i.e.,  $\|\nabla f(\mathbf{X}) - \nabla f(\mathbf{Y})\|_F^2 \leq \rho \|\mathbf{X} - \mathbf{Y}\|_F^2$  for any  $\mathbf{X}$  and  $\mathbf{Y}$ ),

$$\phi(\mathbf{X}) = \sum_{i=1}^{I_2} \kappa(\sigma_i(\mathbf{X})) \quad (3)$$

is the nonconvex regularizer, and  $\kappa$  is the nonconvex penalty satisfying Assumption 1. Some popular choices of  $\kappa$  are, capped- $\ell_1$   $\kappa(\sigma_i(\mathbf{X})) = \log(\frac{1}{\theta} \sigma_i(\mathbf{X}) + 1)$  and LSP  $\kappa(\sigma_i(\mathbf{X})) = \min(\sigma_i(\mathbf{X}), \theta)$ , where  $\theta > 0$  is a constant. More examples are in Appendix ??.

**Assumption 1.**  $\kappa(\alpha)$  is a concave, nondecreasing and  $L$ -Lipschitz continuous function on  $\alpha \geq 0$  with  $\kappa(0) = 0$ .

Recently, the proximal algorithm (Parikh and Boyd 2013) has been used to solve the nonconvex optimization problem in (2), with convergence to a critical point (Lu et al. 2016; Yao et al. 2018). At iteration  $t$ , it produces the iterate

$$\mathbf{X}_{t+1} = \text{prox}_{\frac{\lambda}{\tau} \phi}(\mathbf{Z}_t), \quad (4)$$

where  $\mathbf{Z}_t = \mathbf{X}_t - \frac{1}{\tau} \nabla f(\mathbf{X}_t)$ ,  $\tau > \rho$  is the stepsize, and

$$\text{prox}_{\frac{\lambda}{\tau} \phi}(\mathbf{Z}) \equiv \text{Arg} \min_{\mathbf{X}} \frac{1}{2} \|\mathbf{X} - \mathbf{Z}\|_F^2 + \frac{\lambda}{\tau} \phi(\mathbf{X}), \quad (5)$$

is the proximal step. For these regularizers, we usually have closed-form solutions on their proximal steps (Lemma 2.1). Thus, a SVD is required to compute the proximal step.

**Lemma 2.1** ((Lu et al. 2016)). *Let the SVD of  $\mathbf{Z} \in \mathbb{R}^{I_1 \times I_2}$  be  $\mathbf{U} \Sigma \mathbf{V}^\top$ . Then  $\text{prox}_{\lambda \phi}(\mathbf{Z}) = \mathbf{U} \text{Diag}(y_1, \dots, y_{I_2}) \mathbf{V}^\top$  where  $y_i = \arg \min_{y \geq 0} \frac{1}{2} (y - \sigma_i(\mathbf{Z}))^2 + \lambda \kappa(y)$ .*

**Matrix Completion: ‘‘Sparse plus Low-rank’’ Structure.** In matrix completion,  $f(\mathbf{X}) \equiv \frac{1}{2} \|P_\Omega(\mathbf{X} - \mathbf{O})\|_F^2$  in (2) (Candès and Recht 2009).  $\mathbf{Z}_t$  then becomes:

$$\mathbf{Z}_t = \mathbf{X}_t - \frac{1}{\tau} P_\Omega(\mathbf{X}_t - \mathbf{O}), \quad (6)$$

where  $\frac{1}{\tau} P_\Omega(\mathbf{X}_t - \mathbf{O})$  is sparse and  $\mathbf{X}_t$  is low-rank. This ‘‘sparse plus low-rank’’ structure can enable the SVD computation to be much more efficient (Mazumder, Hastie, and Tibshirani 2010; Yao et al. 2018). Specifically, to compute the SVD of  $\mathbf{Z}_t$  with the power method, most of the efforts are on computing multiplications of the form  $\mathbf{Z}_t \mathbf{b}$  (where  $\mathbf{b} \in \mathbb{R}^{I_1}$ ) and  $\mathbf{a}^\top \mathbf{Z}_t$  (where  $\mathbf{a} \in \mathbb{R}^{I_2}$ ). Let  $\mathbf{X}_t$  be low-rank factorized as  $\mathbf{U}_t \mathbf{V}_t^\top$ . Using (6),

$$\mathbf{Z}_t \mathbf{b} = \mathbf{U}_t (\mathbf{V}_t^\top \mathbf{b}) - \frac{1}{\tau} P_\Omega(\mathbf{Y}_t - \mathbf{O}) \mathbf{b}. \quad (7)$$

This takes  $O((I_1 + I_2)k_t + \|\Omega\|_1)$  time, where  $k_t$  is the rank of  $\mathbf{X}_t$ . Usually,  $k_t \ll I_2$  and  $\|\Omega\|_1 \ll I_1 I_2$ . Thus, it is much faster than direct multiplying  $\mathbf{Z}_t$  and  $\mathbf{b}$ , which takes  $O(I_1 I_2)$  time. The same also holds for  $\mathbf{a}^\top \mathbf{Z}_t$ . Similarly, the proximal step takes  $O((I_1 + I_2)k_t k_{t+1} + \|\Omega\|_1 k_{t+1})$  time, while a direct computation without utilizing the ‘‘sparse plus low-rank’’ structure takes  $O(I_1 I_2 k_{t+1})$  time. Besides, as only  $P_\Omega(\mathbf{X}_t)$  and the factorized form of  $\mathbf{X}_t$  need to be kept, the space requirement is reduced from  $O(I_1 I_2)$  to  $O((I_1 + I_2)k_t + \|\Omega\|_1)$ .

### 2.2 Low-rank Tensor Learning

The nuclear norm has been popularly used in low-rank matrix learning. Recently, it has been extended to the learning of low-rank tensors (Tomioka, Hayashi, and Kashima 2010; Signoretto et al. 2011). The most commonly used low-rank tensor regularizer is the (convex) overlapped nuclear norm, which has better empirical performance than both others variants of nuclear norm for tensor and tensor factorization approaches (Tomioka, Hayashi, and Kashima 2010; Liu et al. 2013; Guo, Yao, and Kwok 2017).

**Definition 1.** (Tomioka, Hayashi, and Kashima 2010) For a  $M$ -order tensor  $\mathcal{X}$ , the overlapped nuclear norm is  $\|\mathcal{X}\|_{\text{overlap}} = \sum_{m=1}^M \lambda_m \|\mathcal{X}_{\langle m \rangle}\|_*$  where  $\lambda_m \geq 0$  are hyperparameters.

Factorization methods, such as the Tucker/CP (Kolda and Bader 2009) and tensor-train decompositions (Oseledets 2011), have also been used for low-rank tensor learning. Compared to nuclear norm regularization, their optimization problems are nonconvex and more difficult, and their empirical performance is often inferior (Tomioka et al. 2011; Liu et al. 2013; Guo, Yao, and Kwok 2017).

### 2.3 Proximal Average (PA) Algorithm

Consider the following problem in some Hilbert space  $\mathcal{H}$ :

$$\min_{\mathbf{x} \in \mathcal{H}} f(\mathbf{x}) + \sum_{i=1}^K \lambda_i g_i(\mathbf{x}), \quad (8)$$

where  $g_i$ s are regularizers. Sometimes, the proximal step for each individual  $g_i$  can be easily computed, but not for  $g(\mathbf{x}) = \sum_{i=1}^K g_i(\mathbf{x})$ . Hence, the proximal algorithm cannot be efficiently used.

Instead, the proximal average (PA) algorithm (Bauschke et al. 2008) generates the next iterate  $\mathbf{x}_{t+1}$  as

$$\mathbf{z}_t = \mathbf{x}_t - \frac{1}{\tau} \nabla f(\mathbf{x}_t), \quad (9)$$

$$\mathbf{y}_{t+1}^i = \text{prox}_{\frac{\lambda_i}{\tau} g_i}(\mathbf{z}_t), \quad i = 1, \dots, K, \quad (10)$$

$$\mathbf{x}_{t+1} = \sum_{i=1}^K \alpha_i \mathbf{y}_{t+1}^i, \quad (11)$$

where  $\alpha_i = \lambda_i / \sum_{i=1}^K \lambda_i$ . As the proximal steps in (10) are easy, the PA algorithm can be significantly faster than the proximal algorithm. When both  $f$  and  $g$  are convex, the PA algorithm converges to an optimal solution of (8) with a proper choice of  $\tau$  (Yu 2013). Recently, the PA algorithm has also been extended to nonconvex  $f$  and  $g_i$ 's (Zhong and Kwok 2014; Yu, Micol, and Xing 2015).

## 3 Proposed Algorithm

In this section, we propose to improve tensor completion performance by reducing penalties for the tensor's top singular values. This is achieved by integrating a nonconvex regularizer with the overlapped nuclear norm.

For 3-order tensors, the completion problem becomes

$$\min_{\mathcal{X}} F(\mathcal{X}) \equiv \frac{1}{2} \|P_{\Omega}(\mathcal{X} - \mathcal{O})\|_F^2 + \sum_{d=1}^D \lambda_d \phi(\mathcal{X}_{\langle d \rangle}), \quad (12)$$

where  $\phi$  is as defined in (3). Note that the regularizer above only sums over  $D \leq M$  modes (instead of  $M$  in Definition 1). This is because in some applications (e.g., those involving color images), the third mode (number of colors) is already small, and so does not need to be low-rank regularized.

When  $D = 1$ , (12) reduces to  $\min_{\mathbf{X} \in \mathbb{R}^{I_1 \times I_2 \times I_3}} \frac{1}{2} \|P_{\Omega}(\mathbf{X} - \mathcal{O}_{\langle 1 \rangle})\|_F^2 + \lambda_1 \phi(\mathbf{X})$ . Thus, this is a matrix completion

problem with nonconvex low-rank regularizer, and can be solved by the proximal algorithm as in (Lu et al. 2016; Yao et al. 2018). When  $\kappa(\alpha)$  in (3) is  $|\alpha|$ , (12) reduces to (convex) overlapped nuclear norm regularization. While  $D$  may not be equal to  $M$ , it can be easily shown that optimization solvers such as alternating direction of multiple multipliers (ADMM) (Tomioka, Hayashi, and Kashima 2010) and fast low-rank tensor completion (FaLRTC) (Liu et al. 2013) can still be used. However, with nonconvex regularization, ADMM no longer has convergence guarantee and the dual in FaLRTC cannot be derived. Factorization-based algorithms, such as gradient descent (Acar et al. 2011) and optimization on Riemannian manifold (Kasai and Mishra 2016), also cannot be used as  $F$  in (12) is not smooth.

### 3.1 First Attempt: Using the PA algorithm

In this section, we show how the PA algorithm for nonconvex regularizers (Zhong and Kwok 2014) can be used to solve (12) when  $D \neq 1$ . First, note that it requires each component nonconvex regularizer of  $g$  (in (8)) to be Lipschitz continuous and admits a difference of convex decomposition. This holds for our  $\phi(\mathbf{X})$  (Yao et al. 2018). Moreover,  $f(\mathcal{X})$  in (8) equals  $\frac{1}{2} \|P_{\Omega}(\mathcal{X} - \mathcal{O})\|_F^2$ . Given the current iterate  $\mathcal{X}_t$ , we have from (9)-(11),

$$\mathcal{Z}_t = \mathcal{X}_t - \frac{1}{\tau} P_{\Omega}(\mathcal{X}_t - \mathcal{O}), \quad (13)$$

$$\mathbf{Y}_{t+1}^i = \text{prox}_{\frac{\lambda_i}{\tau} \phi}([\mathcal{Z}_t]_{\langle i \rangle}), \quad i = 1, \dots, D, \quad (14)$$

$$\mathcal{X}_{t+1} = \sum_{i=1}^D \alpha_i (\mathbf{Y}_{t+1}^i)^{\langle i \rangle}. \quad (15)$$

The proximal step in (14) requires SVD on the unfolded  $\mathcal{Z}_t$ , while (15) requires the folding of  $\mathbf{Y}_{t+1}^i$ . A direct implementation of (13)-(15) takes a space complexity of  $O(I_{\times})$  and an iteration time complexity of  $O(I_{\times} \sum_{i=1}^D I_i)$ , where  $I_{\times} = \prod_{i=d}^3 I_d$  and  $I_{+} = \sum_{i=d}^3 I_d$ , and is expensive.

### 3.2 Cheap Iterations: Utilizing problem structure

As discussed in Section 2.1, the ‘‘sparse plus low-rank’’ structure can significantly speed up the proximal algorithm for matrix completion. Here, we attempt to use a similar structure, in the tensor setting.

**Using the ‘‘Sparse plus Low-Rank’’ Structure.** Let  $\mathbf{Y}_t^i$  be factorized as  $\mathbf{Y}_t^i = \mathbf{U}_t^i (\mathbf{V}_t^i)^{\top}$ . From (13) and (15),

$$\mathcal{Z}_t = \sum_{i=1}^D \alpha_i (\mathbf{U}_t^i (\mathbf{V}_t^i)^{\top})^{\langle i \rangle} - \frac{1}{\tau} P_{\Omega}(\mathcal{X}_t - \mathcal{O}), \quad (16)$$

where  $\sum_{i=1}^D \alpha_i (\mathbf{U}_t^i (\mathbf{V}_t^i)^{\top})^{\langle i \rangle}$  is a sum of low-rank matrices, and  $\frac{1}{\tau} P_{\Omega}(\mathcal{X}_t - \mathcal{O})$  is a sparse tensor. Thus,  $\mathcal{Z}_t$  also has a ‘‘sparse plus low-rank’’ structure.

To compute the proximal step in (14), recall that we have to perform matrix multiplications of the form  $(\mathcal{Z}_t)_{\langle i \rangle} \mathbf{b}$  (with

$\mathbf{b} \in \mathbb{R}^{I_\times/I_i}$  and  $\mathbf{a}^\top (\mathcal{Z}_t)_{\langle i \rangle}$  (with  $\mathbf{a} \in \mathbb{R}^{I_i}$ ). Using (16),

$$\begin{aligned} (\mathcal{Z}_t)_{\langle i \rangle} \mathbf{b} &= \alpha_i \mathbf{U}_t^i [(\mathbf{V}_t^i)^\top \mathbf{b}] + \sum_{j \neq i} \alpha_j \left( [(\mathbf{U}_t^j (\mathbf{V}_t^j)^\top)^{\langle j \rangle}]_{\langle i \rangle} \mathbf{b} \right) \\ &\quad - \frac{1}{\tau} [P_\Omega(\mathcal{X}_t - \mathcal{O})]_{\langle i \rangle} \mathbf{b}. \end{aligned} \quad (17)$$

Similarly, for  $\mathbf{a}^\top (\mathcal{Z}_t)_{\langle i \rangle}$ ,

$$\begin{aligned} \mathbf{a}^\top (\mathcal{Z}_t)_{\langle i \rangle} &= \alpha_i (\mathbf{a}^\top \mathbf{U}_t^i) (\mathbf{V}_t^i)^\top + \sum_{j \neq i} \alpha_j \left( \mathbf{a}^\top [(\mathbf{U}_t^j (\mathbf{V}_t^j)^\top)^{\langle j \rangle}]_{\langle i \rangle} \right) \\ &\quad - \frac{1}{\tau} \mathbf{a}^\top [P_\Omega(\mathcal{X}_t - \mathcal{O})]_{\langle i \rangle}, \end{aligned} \quad (18)$$

The first terms in (17) and (18) can be directly computed, and take  $O((I_\times/I_i + I_i)k_t^i)$  space and time, where  $k_t^i$  is the rank of  $\mathbf{Y}_t^i$ . However, the other terms need more careful consideration in order to be efficient.

**Computing  $[P_\Omega(\mathcal{X}_t - \mathcal{O})]_{\langle i \rangle} \mathbf{b}$  and  $\mathbf{a}^\top [P_\Omega(\mathcal{X}_t - \mathcal{O})]_{\langle i \rangle}$ .** A direct computation involves unfolding, which takes  $O(I_\times)$  space and time. In the following, we avoid unfolding by computing only the observed elements from the low-rank factorizations of  $\mathbf{Y}_t^i$ 's in (14), and then use sparse tensor multiplications.

To efficiently process the sparse tensor  $P_\Omega(\mathcal{X}_t - \mathcal{O})$ , we use the popular coordinate format (Bader and Kolda 2007). Its  $p$ th observed element with value  $v_p$  is represented as  $\{i_p^1, i_p^2, i_p^3, v_p\}$ , where  $\{i_p^1, i_p^2, i_p^3\}$  indexes positions in each mode. Using  $\mathbf{Y}_t^i = \mathbf{U}_t^i (\mathbf{V}_t^i)^\top$ , each observed element in  $P_\Omega(\mathcal{X}_t - \mathcal{O})$  can be computed by Algorithm 1. Construction of the whole  $P_\Omega(\mathcal{X}_t - \mathcal{O})$  then takes  $O(\|\Omega\|_1 \sum_{i=1}^D k_t^i)$  time. We then use sparse tensor packages (such as the Tensor Toolbox in (Bader and Kolda 2007)) to compute  $[P_\Omega(\mathcal{X}_t - \mathcal{O})]_{\langle i \rangle} \mathbf{b}$  and  $\mathbf{a}^\top [P_\Omega(\mathcal{X}_t - \mathcal{O})]_{\langle i \rangle}$ , which takes  $O(\|\Omega\|_1)$  space and time.

---

**Algorithm 1** Computing the  $p$ th element in  $P_\Omega(\mathcal{X}_t - \mathcal{O})$ .

---

**Require:** index  $\{i_p^1, i_p^2, i_p^3\}$ , factorizations of  $\mathbf{Y}_t^1, \mathbf{Y}_t^2, \mathbf{Y}_t^3$ ;  
1:  $\mathbf{u}_1 \leftarrow$  the  $i_p^1$ th row of  $\mathbf{U}_t^1$ ;  
2:  $\mathbf{v}_1 \leftarrow$  the  $(i_p^2 I_2 + i_p^3)$ th row of  $\mathbf{V}_t^1$ ;  
3:  $\mathbf{u}_2 \leftarrow$  the  $i_p^2$ th row of  $\mathbf{U}_t^2$ ;  
4:  $\mathbf{v}_2 \leftarrow$  the  $(i_p^3 I_3 + i_p^1)$ th row of  $\mathbf{V}_t^2$ ;  
5: **if**  $D = 3$  **then**  
6:    $\mathbf{u}_3 \leftarrow$  the  $i_p^3$ th row of  $\mathbf{U}_t^3$ ;  
7:    $\mathbf{v}_3 \leftarrow$  the  $(i_p^1 I_1 + i_p^2)$ th row of  $\mathbf{V}_t^3$ ;  
8: **end if**  
9:  $o_p \leftarrow$   $p$ th element in  $P_\Omega(\mathcal{O})$ ;  
10: **return**  $v_p = \sum_{i=1}^D \alpha_i \mathbf{u}_i^\top \mathbf{v}_i - o_p$ .

---

**Computing  $\mathbf{a}^\top [(\mathbf{U}_t^i (\mathbf{V}_t^i)^\top)^{\langle j \rangle}]_{\langle i \rangle}$  and  $[(\mathbf{U}_t^i (\mathbf{V}_t^i)^\top)^{\langle j \rangle}]_{\langle i \rangle} \mathbf{b}$ .** These terms involve folding and unfolding operations. A direct computation will take  $O(I_\times)$  space and  $O(k_t^i I_\times)$  time. The following Proposition shows that these products can be computed more efficiently without folding and unfolding.

**Proposition 3.1.** *Let  $\{\pi_1, \pi_2, \pi_3\}$  be any permutation of  $\{1, 2, 3\}$ ,  $\mathbf{U} \in \mathbb{R}^{I_{\pi_1} \times k}$ ,  $\mathbf{V} \in \mathbb{R}^{I_{\pi_2} I_{\pi_3} \times k}$ , and  $\mathbf{u}_p$  (resp.  $\mathbf{v}_p$ )*

*be the  $p$ th column in  $\mathbf{U}$  (resp.  $\mathbf{V}$ ). For any  $\mathbf{a} \in \mathbb{R}^{I_{\pi_1}}$  and  $\mathbf{b} \in \mathbb{R}^{I_{\pi_2} I_{\pi_3}}$ , we have*

- (i).  $\mathbf{a}^\top [(\mathbf{U}\mathbf{V}^\top)^{\langle \pi_1 \rangle}]_{\langle \pi_2 \rangle} = \sum_{p=1}^k \mathbf{u}_p^\top \otimes [\mathbf{a}^\top \text{mat}(\mathbf{v}_p)]$  and,
- (ii).  $[(\mathbf{U}\mathbf{V}^\top)^{\langle \pi_1 \rangle}]_{\langle \pi_2 \rangle} \mathbf{b} = \sum_{p=1}^k \text{mat}(\mathbf{v}_p) \text{mat}(\mathbf{b})^\top \mathbf{u}_p$ .

where  $\otimes$  is the Kronecker product, and  $\text{mat}(\mathbf{c})$  reshapes vector  $\mathbf{c} \in \mathbb{R}^{I_{\pi_1} I_{\pi_2}}$  into a  $I_{\pi_1} \times I_{\pi_2}$  matrix.

Taking  $\pi_1 = j$  and  $\pi_2 = i$  in Proposition 3.1,  $\mathbf{a}^\top \text{mat}(\mathbf{v}_p)$  takes  $O(I_\times/I_i)$  space and time, and the Kronecker product takes  $O(I_\times/I_j)$  space and time. Thus, computation of  $\mathbf{a}^\top [(\mathbf{U}_t^i (\mathbf{V}_t^i)^\top)^{\langle j \rangle}]_{\langle i \rangle}$  takes a total of  $O((1/I_i + 1/I_j)k_t^i I_\times)$  time and  $O(I_\times/I_i + I_\times/I_j)$  space. The same holds for the computation of  $[(\mathbf{U}_t^i (\mathbf{V}_t^i)^\top)^{\langle j \rangle}]_{\langle i \rangle} \mathbf{b}$ .

**Total Complexity.** Combining the above complexities, and noting that we have to keep the factorized form  $\mathbf{U}_t^i (\mathbf{V}_t^i)^\top$  of  $\mathbf{Y}_t^i$ , computing (17) and (18) take  $O(\sum_{j \neq i} (1/I_i + 1/I_j)k_t^i I_\times + \|\Omega\|_1)$  space and time. As (14) performs  $D$  proximal steps, plugging techniques here into (13)-(15), the resulting algorithm takes a total of

$$O\left(\sum_{i=1}^D \sum_{j \neq i} \left(\frac{1}{I_i} + \frac{1}{I_j}\right) k_t^i I_\times + \|\Omega\|_1\right), \quad (19)$$

space and

$$O\left(\sum_{i=1}^D \sum_{j \neq i} \left(\frac{1}{I_i} + \frac{1}{I_j}\right) k_t^i k_{t+1}^i I_\times + \|\Omega\|_1 (k_t^i + k_{t+1}^i)\right), \quad (20)$$

time for each iteration. As  $k_t^i, k_{t+1}^i \ll I_i$ , these are much lower than those of a direct implementation in Section 3.1.

### 3.3 Speedup Convergence

**Using Acceleration.** The PA algorithm uses only first-order information, and may suffer slow convergence (Parikh and Boyd 2013). To address this problem, we adopt the popularly used Nesterov acceleration (Nesterov 1983). Note that it has not been used before with the PA algorithm on nonconvex optimization. We adopt the acceleration scheme in (Yao et al. 2017) here, and the resultant procedures are shown in Algorithm 2. Note that, techniques in Section 3.2 can still be used, we only need to keep sparse tensors  $P_\Omega(\mathcal{O})$  and  $P_\Omega(\mathcal{V}_t)$ , and factorized forms of  $\mathbf{Y}_{t+1}^i$  during the iterating. No dense tensors need to be explicitly formed. Thus, while  $\mathcal{Y}_t$  is more complex than  $\mathcal{X}_t$ , it still has the special ‘‘sparse plus low-rank’’ structure (details are in Appendix B). The iteration time and complexity of Algorithm 2 are still in (19) and (20). As a result, ‘‘sparse plus low-rank’’ structure can still be preserved with acceleration, and we can achieve both fast convergence and cheap iterations.

**Convergence Analysis.** While the Nesterov acceleration (Nesterov 1983) has been popularly used, it has not been used with the PA algorithm on nonconvex optimization. Thus, previous proofs cannot be directly used here. The following from (Zhong and Kwok 2014) shows the proximal step in (14) implicitly produces an new regularizer  $\tilde{g}_\tau$ .

---

**Algorithm 2** Fast Tensor Completion with Nonconvex Regularization (FasTer) algorithm.

---

```

1: initialize  $\mathcal{X}_0 = \mathcal{X}_1 = 0$  and stepsize  $\tau > (\rho + DL)$ ;
2: for  $t = 1, \dots, T$  do
3:    $\mathcal{Y}_t = \mathcal{X}_t + \frac{t-1}{t+2}(\mathcal{X}_t - \mathcal{X}_{t-1})$ ;
4:   if  $F_\tau(\mathcal{Y}_t) \leq F_\tau(\mathcal{X}_t)$  then
5:      $\mathcal{V}_t = \mathcal{Y}_t$ ;
6:   else
7:      $\mathcal{V}_t = \mathcal{X}_t$ ;
8:   end if
9:    $\mathcal{Z}_t = \mathcal{V}_t - \frac{1}{\tau}P_\Omega(\mathcal{V}_t - \mathcal{O})$ ;
10:  for  $i = 1, \dots, D$  do
11:     $\mathbf{X}_{t+1}^i = \text{prox}_{\frac{\lambda_i}{\tau} \phi}(\mathcal{Z}_t)_{\langle i \rangle}$ ;
12:  end for
13:   $\mathcal{X}_{t+1} = \sum_{i=1}^D \alpha_i (\mathbf{Y}_{t+1}^i)^{\langle i \rangle}$ ; // construct implicitly
14: end for
15: return  $\mathcal{X}_{T+1}$ .
```

---

**Proposition 3.2.** *There exists a function  $\bar{g}_\tau$  such that  $\text{prox}_{\bar{g}_\tau}(\mathcal{Z}) = \sum_{i=1}^D \alpha_i \text{prox}_{\frac{\lambda_i}{\tau} \phi}([\mathcal{Z}]_{\langle i \rangle})$  for any  $\tau > 0$ .*

The following bounds the difference between the optimal values of the objectives  $F(\mathcal{X})$  in (12) and  $F_\tau(\mathcal{X}) \equiv \frac{1}{2} \|P_\Omega(\mathcal{X} - \mathcal{O})\|_F^2 + \bar{g}_\tau(\mathcal{X})$ .

**Proposition 3.3.**  $0 \leq \min F - \min F_\tau \leq \frac{1}{\tau} \sum_{i=1}^D \alpha_i L^2$ .

**Theorem 3.4.** *The sequence  $\{\mathcal{X}_t\}$  generated from Algorithm 2 has at least one limit point, and all limit points are critical points of  $F_\tau(\mathcal{X})$ .*

Combining Theorem 3.4 with Proposition 3.3, we can see that a larger  $\tau$  leads to better approximation to the original problem  $F$ . However, it also leads to smaller steps, and slower convergence. In the experiments, we set  $\tau = 1$ ; besides, since  $F_\tau$  is hard to evaluate, and so we use  $F$  instead as in (Zhong and Kwok 2014). Finally, while Theorem 3.4 provides no convergence rate, empirically the accelerated algorithm is significantly faster than its non-accelerated version (Section 4.1).

## 4 Experiments

Experiments are performed on a PC with Intel i7 CPU and 32GB memory. All algorithms are implemented in Matlab, except operations on sparse tensor and matrix are implemented in C and linked to Matlab by mex files.

### 4.1 Synthetic Data

In the synthetic data, we consider two cases, i.e.,  $D = 2$  and 3 in (12). The difference is that, when  $D = 2$ , the low-rank regularizations are imposed on the first two unfolding matrices from  $\mathcal{X}$  but not the third one.

We follow the setup suggested in (Song et al. 2017). The synthetic data is generated as  $^2 \bar{\mathcal{O}} = \sum_{i=1}^5 s_i (\mathbf{a}_i \circ \mathbf{b}_i \circ \mathbf{c}_i)$  where  $\mathbf{a}_i \in \mathbb{R}^{I_1}$ ,  $\mathbf{b}_i \in \mathbb{R}^{I_2}$  and  $\mathbf{c}_i \in \mathbb{R}^{I_3}$ . All the elements in  $\mathbf{a}_i$ s,  $\mathbf{b}_i$ s,  $\mathbf{c}_i$ s and  $s_i$ s are sampled independently from Gaussian distribution  $\mathcal{N}(0, 1)$ . A total

<sup>2</sup>We follow (Kolda and Bader 2009), and  $\circ$  denotes out products with  $[\mathbf{a} \circ \mathbf{b} \circ \mathbf{c}]_{ijk} = a_i b_j c_k$ .

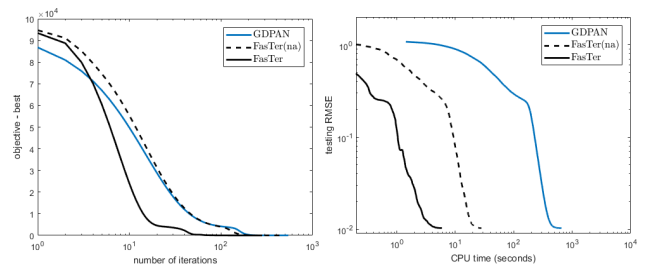
number of  $\|\bar{\Omega}\|_1 = I_+ I_3 \log(I_+)/5$  elements are uniform randomly observed from  $\bar{\mathcal{O}} = \bar{\mathcal{O}} + \mathcal{N}$ , where  $\mathcal{N}$  is the noise sampled independently from  $\mathcal{N}(0, 0.01)$ . We use 50% of the observations for training, the remained 50% for validation, and the testing is performed on the remain unobserved elements in  $\bar{\mathcal{O}}$ .

Three nonconvex penalties as examples here, i.e., capped- $\ell_1$  norm (Zhang 2010a), LSP (Candès, Wakin, and Boyd 2008) and TNN (Hu et al. 2013). Following (Lu et al. 2016; Yao et al. 2018; Yao et al. 2017), the recovery performance is measured by (i) root-mean-square-error (RMSE):  $\text{RMSE} = \|P_{\bar{\Omega}}(\mathcal{X} - \bar{\mathcal{O}})\|_F / \sqrt{\|\bar{\Omega}\|_1}$ , where  $\mathcal{X}$  is the low-rank tensor recovered from different algorithms, and  $\bar{\Omega}$  denotes the unobserved elements in  $\bar{\mathcal{O}}$ ; and (ii). running CPU time.

We compare different variants of PA algorithm for the overlapped regularization here, as it is the only algorithm solving (12) with convergence guarantee. Thus, the following algorithms are compared (i). GDPAN (Zhong and Kwok 2014): plain PA algorithm for nonconvex problem (12); (ii). The proposed Algorithm 2 (denoted as FasTer), which utilizing acceleration, the ‘‘sparse plus low-rank’’ structure, and Proposition 3.1 in computing the proximal step; (iii). Variant of FasTer without acceleration (denoted as FasTer(na)); and (iv). Finally, PA-APG (Yu 2013): accelerated PA algorithm for the convex overlapped nuclear norm is used as a baseline.

**Case (i): Small  $I_3$ .** We take  $I_1 = I_2 = 25c_1$ ,  $I_3 = 5$  and vary  $c_1 = \{50, 100\}$  here. Experiments are repeated five times. Recovery performance is in <sup>3</sup> Table 1. We can see that PA-APG, which is based on the convex overlapping nuclear norm, has much higher testing RMSEs than, GDPAN, FasTer(na) and FasTer, which are based on the nonconvex regularization. Besides, three nonconvex penalties, i.e., capped- $\ell_1$ , LSP and TNN, have the similar empirical performance. This is also observed in (Lu et al. 2016; Yao et al. 2017; Yao et al. 2018).

The convergence of testing RMSE and objective value are in Figure 1. First, we can see that both PA-APG and GDPAN are very slow. Then, when measured by the number of iterations, FasTer(na) converges as fast as GDPAN. However, when measured by CPU time, FasTer(na) becomes much faster than GDPAN, as it utilizes the special ‘‘sparse plus low-rank’’ structure on computing the proximal steps. TNCR is even faster than FasTer(na) due to acceleration.



(a) objective v.s. iterations. (b) testing RMSE v.s. time.

Figure 1: Convergence of testing RMSE on synthetic data (Case (i)) and  $c = 1000$ , and capped- $\ell_1$  is used.

<sup>3</sup>The best and comparable performances (according to the pairwise t-test with 95% confidence) are highlighted.

Table 1: Testing RMSE (scaled by  $10^{-2}$ ) and CPU time (in seconds) of various algorithms on synthetic data. The left part is for Case (i), and the right part is for Case (ii).

		$c_1 = 50$ , nnz:5.64%		$c_1 = 100$ , nnz: 3.09%		$c_2 = 20$ , nnz:4.77%		$c_2 = 40$ , nnz:2.70%	
		RMSE	time (sec)	RMSE	time (sec)	RMSE	time (sec)	RMSE	time (sec)
convex	PA-APG	1.41±0.12	257.2±34.8	1.49±0.11	2131.7±419.9	1.10±0.07	250.1±59.6	0.98±0.01	6196.4±2033.4
nonconvex (capped- $\ell_1$ )	GDPAN	<b>1.03±0.01</b>	64.4±29.5	<b>1.03±0.01</b>	665.4±99.8	<b>0.10±0.01</b>	179.9±21.5	<b>0.06±0.01</b>	3670.4±225.8
	FasTer(na)	<b>1.03±0.01</b>	7.1±4.5	<b>1.03±0.01</b>	27.9±5.1	<b>0.10±0.01</b>	22.9±1.1	<b>0.06±0.01</b>	575.9±70.9
	FasTer	<b>1.03±0.01</b>	<b>2.1±1.4</b>	<b>1.03±0.01</b>	<b>5.9±1.6</b>	<b>0.09±0.01</b>	5.1±0.3	<b>0.06±0.01</b>	89.4±13.4
nonconvex (LSP)	GDPAN	<b>1.03±0.01</b>	59.1±26.4	1.04±0.01	654.1±214.7	<b>0.10±0.01</b>	177.8±16.4	<b>0.06±0.01</b>	3794.0±419.5
	FasTer(na)	<b>1.03±0.01</b>	4.5±1.5	1.04±0.01	27.9±5.7	<b>0.10±0.01</b>	21.8±0.8	<b>0.06±0.01</b>	544.2±75.5
	FasTer	<b>1.03±0.01</b>	<b>1.6±1.1</b>	1.04±0.01	<b>5.8±2.8</b>	<b>0.10±0.01</b>	4.6±0.7	<b>0.06±0.01</b>	81.3±24.9
nonconvex (TNN)	GDPAN	1.04±0.01	69.3±26.4	1.04±0.01	615.0±140.9	<b>0.10±0.01</b>	184.1±17.7	<b>0.06±0.01</b>	3922.9±280.1
	FasTer(na)	1.04±0.01	6.6±3.8	1.04±0.01	26.2±4.0	<b>0.10±0.01</b>	21.8±0.9	<b>0.06±0.01</b>	554.7±44.1
	FasTer	1.04±0.01	<b>1.4±0.3</b>	<b>1.03±0.01</b>	<b>5.3±1.5</b>	<b>0.10±0.01</b>	4.8±0.4	<b>0.06±0.01</b>	78.0±9.4

**Case (ii): Large  $I_3$ .** Here we take  $I_1 = I_2 = I_3 = 10c_2$ , and vary  $c_2 = \{20, 40\}$  here. Experiments are repeated five times. Results are in Table 1. Again, we can see capped- $\ell_1$  norm, LSP and TNN, have the same testing RMSE. GDPAN, FasTer(na) and FasTer, all have much lower testing RMSEs than PA-APG. Convergence of testing RMSE and objective value are in Figure 2. Again, FasTer(na) is much faster than GDPAN due to Section 3.2. Besides, FasTer is the fastest due to utilization of special structure and acceleration.

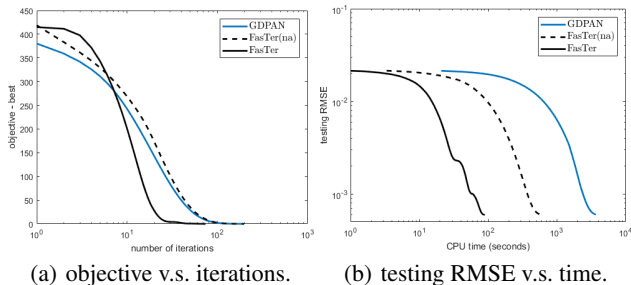


Figure 2: Convergence of testing RMSE on synthetic data (Case (ii)) with  $c = 400$ , and capped- $\ell_1$  is used.

**Comparison of Case (i) and (ii).** Here, we examine the difference of  $D = 2$  and 3 in (12) on above case (i) and (ii). Only FasTer is considered here due to its efficiency. The performance is compared in Table 2. For case (i), we can see that  $D = 2$  and 3 can achieve the same testing RMSEs. However,  $D = 3$  leads to much longer CPU time than  $D = 2$ . This is due to  $I_3$  is small, the low-rank assumption cannot hold on the third mode and  $k_3^t \ll I_3$  does not hold. Thus, the proximal step for the third mode (i.e.,  $i = 3$  for step 11 in Algorithm 2) is much more expensive than these for the first two modes. For case (ii), on CPU time, as  $D = 3$  has one more low-rank regularization than the  $D = 2$ , it is slightly more expensive. However, on testing RMSE, the performance obtained from  $D = 2$  is much worse than  $D = 3$ , which results from FasTer with  $D = 2$  cannot capture the low-rank property on the third mode.

## 4.2 Real Data sets

In the sequel, based on above observations, we use  $D = 2$  in (12) if  $I_3$  is very small (i.e.,  $I_3 \leq 10$  empirically), otherwise we use  $D = 3$ ; besides, as all three nonconvex penalty functions have similar performance, only LSP is considered. All experiments are repeated five times in the sequel.

Three types of algorithms are used for comparison here.

(i). *Convex models*, including, ADMM (Tomioka, Hayashi,

Table 2: Comparison of FasTer with different  $D$  used in (12) on the synthetic data with case (i) and (ii). Testing RMSEs are scaled by  $10^{-2}$  and CPU time is in seconds.

	$D$	case (i), $c_1 = 100$		case (ii), $c_2 = 40$	
		RMSE	time (sec)	RMSE	time (sec)
capped- $\ell_1$	2	<b>1.03±0.01</b>	<b>5.9±1.6</b>	0.09±0.001	<b>40.0±1.9</b>
	3	<b>1.03±0.01</b>	918.7±500.9	<b>0.06±0.01</b>	89.4±13.4
LSP	2	1.04±0.01	<b>5.8±2.8</b>	0.10±0.01	<b>50.8±27.2</b>
	3	<b>1.03±0.01</b>	899.7±404.4	<b>0.06±0.01</b>	81.3±24.9
TNN	2	<b>1.03±0.01</b>	<b>5.3±1.5</b>	0.09±0.01	<b>39.3±14.3</b>
	3	1.04±0.01	615.5±388.3	<b>0.06±0.01</b>	78.0±9.4

and Kashima 2010), FaLRTC (Liu et al. 2013), PA-APG (Yu 2013), FFW (Guo, Yao, and Kwok 2017) and TNN (Zhang and Aeron 2017); (ii). *Factorization approaches*, including, RP (Kasai and Mishra 2016), TMac (Xu et al. 2013), CP-WOPT (Acar et al. 2011) and TMac-TT (Bengua et al. 2017). (iii). Finally, *nonconvex regularization*, including GDPAN (Zhong and Kwok 2014) and the proposed FasTer (Algorithm 2). FasTer(na) in Section 4.1 is not used as it is a slower variant of FasTer. Due to lack of space, we put a more complete comparison of above algorithms in Appendix ??.

**Color Image.** We use the images, i.e., *windows*, *tree* and *rice*, from (Guo, Yao, and Kwok 2017; Hu et al. 2013). We resize size of all images to  $1000 \times 1000 \times 3$  it here in order to make a decomposition for TMac-TT algorithm. Images are show in Appendix ?? . We normalize each pixels into range  $[0, 1]$ . We randomly sample 10% of all the pixels for training, and add Gaussian noise  $\mathcal{N}(0, 0.01)$  to them. Half of the ratings for training are used for validation. The rest unseen clean pixels are used for testing. Performance of various algorithms are measured by RMSE on the testing pixels and the CPU time.

Testing RMSEs are in Table 3. We can see that GDPAN and FasTer achieves similar testing RMSE, and are much lower than both convex regularization (ADMM, FaLRTC, PA-APG, FFW and TNN) and factorization approach (RP, TMac, CP-OPT, TMac-TT). This again verifies that nonconvex regularization offers better empirical performance than the other approaches.

Convergence of testing RMSE vs CPU time is in Figure 3. It shows that FFW and RP are very fast but their testing RMSEs are much higher than that of FasTer. FasTer solves the same optimization problem as GDPAN, thus they have same testing RMSE. However, by utilizing the “sparse plus low-rank” structure and acceleration, FasTer is much more efficient than GDPAN, and is comparable with FFW and RP.

Table 3: Testing RMSEs of algorithms on color images.

		<i>windows</i>	<i>tree</i>	<i>rice</i>
convex	ADMM	0.661±0.006	0.615±0.003	0.526±0.003
	FaLRTC	0.559±0.014	0.576±0.004	0.489±0.006
	PA-APG	0.561±0.007	0.593±0.021	0.485±0.009
	FFW	0.774±0.006	0.629±0.003	0.598±0.004
	TNN	0.567±0.005	0.647±0.004	0.561±0.004
factorization	RP	0.450±0.021	0.518±0.010	0.568±0.028
	TMac	1.313±0.005	1.922±0.003	1.748±0.005
	CP-OPT	0.911±0.122	0.823±0.092	0.704±0.057
	TMac-TT	1.118±0.104	0.740±0.033	0.682±0.086
ncvx	GDPAN	<b>0.305±0.004</b>	<b>0.467±0.002</b>	0.505±0.005
	FasTer	<b>0.304±0.002</b>	<b>0.467±0.005</b>	<b>0.390±0.003</b>

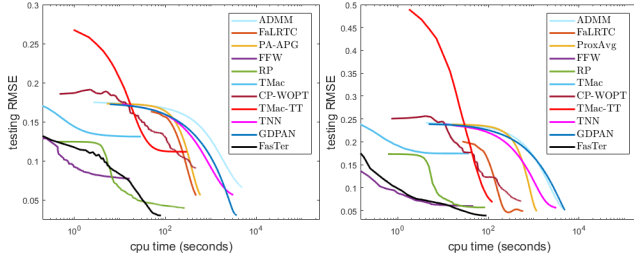


Figure 3: Testing RMSE v.s CPU time (seconds) various on the color image *windows* and *tree*.

**Hyper-Spectrum Image.** Experiments are performed on three hyper-spectral images, i.e., *Cabbage* (1312×432×49), *Scene* (1312×951×49) and *Female* (592×409×148). Their details are in Appendix ???. The third dimension denotes the bands of images. We use the same setup as for the color image. ADMM, TNN, GDPAN are not compared as they are too slow; TMac-TT is also not compared as its initialization cannot be done in 12 hours (Appendix ??).

Performance is shown in Table 4. Again, we can see that, as nonconvex regularizations can less penalize large singular values, FasTer can achieve much lower testing RMSE than both convex and factorization based approaches. Testing RMSE v.s. CPU time is shown in Figure 4. The lowest RMSE is offered by FasTer, and it is much faster than all other approaches except for TMac and FFW. While TMac and FFW are very fast, their testing RMSEs are much higher than that of FasTer. Thus, FasTer is very efficient and offers good empirical performance.

Table 4: Testing RMSEs (scaled by  $10^{-3}$ ) of various algorithms on hyperspectral images.

		<i>Cabbage</i>	<i>Scene</i>	<i>Female</i>
convex	FaLRTC	10.50±0.12	23.08±0.24	13.33±0.04
	PA-APG	9.04±0.04	23.69±0.24	11.57±0.03
	FFW	9.62±0.04	18.89±0.08	20.96±0.06
factorization	RP	4.67±0.11	19.61±0.05	6.47±0.03
	TMac	48.73±0.59	60.06±0.08	198.97±0.06
	CP-OPT	24.17±4.24	49.54±3.01	19.75±1.44
ncvx	FasTer	<b>3.79±0.12</b>	<b>16.40±0.01</b>	<b>5.93±0.14</b>

**Social Networks.** Finally, we perform experiments on the *YouTube* data set (Lei, Wang, and Liu 2009). It contains 15,088 users, and describes five types of user interactions. Thus, it forms a  $15088 \times 15088 \times 5$  tensor, with a total of 27,257,790 nonzero elements. Following (Guo, Yao, and Kwok 2017), we formulate multi-relational link prediction as a tensor completion problem. Here, we perform

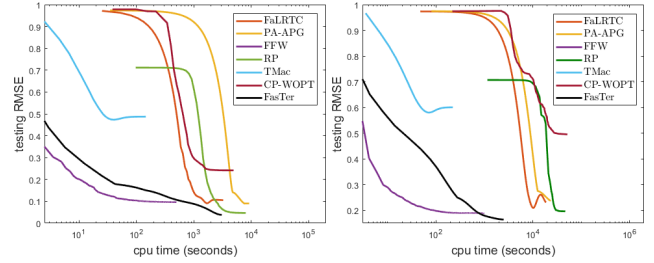


Figure 4: Testing RMSE vs CPU time (minutes) on hyper-spectral image *Cabbage* and *Scene*.

experiments on both a small *YouTube* subset, which is obtained by random selecting 1000 users (leading to 12,101 observations), and the full *Youtube* dataset. We use 50% of the observations for training, another 25% for validation and the remaining for testing.

Experiments are repeated five times. Testing RMSEs are in Table 5 and testing RMSE v.s. CPU time is in Figure 5. In these datasets, we can see FasTer not only achieves lower testing RMSEs but also runs much faster than other algorithms. This again demonstrates that FasTer is very efficient and offers good empirical performance.

Table 5: Testing RMSEs on *Youtube* data set. FaLRTC, PA-APG and CP-OPT are too slow, thus are not run on full set.

		subset	full set
convex	FaLRTC	0.622±0.060	—
	PA-APG	0.659±0.047	—
	FFW	0.626±0.054	0.395±0.001
factorization	RP	0.554±0.026	0.410±0.001
	TMac	0.807±0.035	0.611±0.007
	CP-OPT	0.667±0.016	—
ncvx	FasTer	<b>0.488±0.017</b>	<b>0.370±0.001</b>

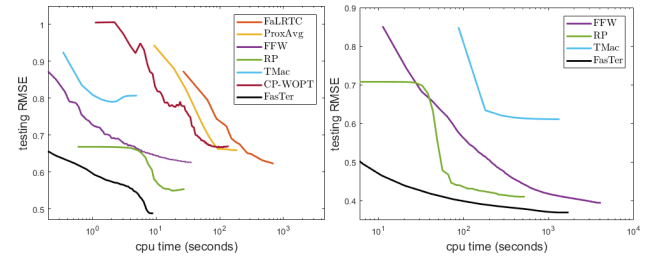


Figure 5: Testing RMSE v.s CPU time (seconds) on *Youtube*.

## 5 Conclusion

In this paper, we propose a new low-rank tensor completion model with nonconvex regularizations. While the nonconvex proximal average (PA) algorithm is the only applicable algorithm, it has large space demand and expensive iteration complexity. To address these problems, we show how proximal steps in PA algorithm can be computed efficiently and how its slow convergence can be sped up with acceleration. The convergence to critical points is of the new algorithm still guaranteed. Finally, experimental comparison of the proposed approach with various other tensor completion approaches demonstrates

that the proposed algorithm is very efficient and nonconvex regularization can produce better empirical performance.

## References

- [Acar et al. 2011] Acar, E.; Dunlavy, D.; Kolda, T.; and Mørup, M. 2011. Scalable tensor factorizations for incomplete data. *Chemometrics and Intelligent Laboratory Systems* 106(1):41–56.
- [Bader and Kolda 2007] Bader, B., and Kolda, T. 2007. Efficient MATLAB computations with sparse and factored tensors. *SIAM Journal on Scientific Computing* 30(1):205–231.
- [Bauschke et al. 2008] Bauschke, H. H.; Goebel, R.; Lucet, Y.; and Wang, X. 2008. The proximal average: basic theory. *JOPT* 19(2):766–785.
- [Bengua et al. 2017] Bengua, J.; Phien, H.; Tuan, H.; and Do, M. 2017. Efficient tensor completion for color image and video recovery: Low-rank tensor train. *TIP* 26(5):2466–2479.
- [Candès and Recht 2009] Candès, E., and Recht, B. 2009. Exact matrix completion via convex optimization. *Foundations of Computational Mathematics* 9(6):717–772.
- [Candès, Wakin, and Boyd 2008] Candès, E.; Wakin, M.; and Boyd, S. 2008. Enhancing sparsity by reweighted  $\ell_1$  minimization. *JFAA* 14(5-6):877–905.
- [Chandrasekaran et al. 2012] Chandrasekaran, V.; Recht, B.; Parrilo, P. A.; and Willsky, A. S. 2012. The convex geometry of linear inverse problems. *Foundations of Computational mathematics* 12(6):805–849.
- [Cheng et al. 2016] Cheng, H.; Yu, Y.; Zhang, X.; Xing, E.; and Schuurmans, D. 2016. Scalable and sound low-rank tensor learning. In *AISTAT*, 1114–1123.
- [Fan and Li 2001] Fan, J., and Li, R. 2001. Variable selection via nonconcave penalized likelihood and its oracle properties. *JASA* 96(456):1348–1360.
- [Gandy, Recht, and Yamada 2011] Gandy, S.; Recht, B.; and Yamada, I. 2011. Tensor completion and low-n-rank tensor recovery via convex optimization. *Inverse Problems* 27(2):025010.
- [Gui, Han, and Gu 2016] Gui, H.; Han, J.; and Gu, Q. 2016. Towards faster rates and oracle property for low-rank matrix estimation. In *ICML*, 2300–2309.
- [Guo, Yao, and Kwok 2017] Guo, X.; Yao, Q.; and Kwok, J. 2017. Efficient sparse low-rank tensor completion using the Frank-Wolfe algorithm. In *AAAI*, 1948–1954.
- [Hu et al. 2013] Hu, Y.; Zhang, D.; Ye, J.; Li, X.; and He, X. 2013. Fast and accurate matrix completion via truncated nuclear norm regularization. *TPAMI* 35(9):2117–2130.
- [Kasai and Mishra 2016] Kasai, H., and Mishra, B. 2016. Low-rank tensor completion: a Riemannian manifold preconditioning approach. In *ICML*, 1012–1021.
- [Kolda and Bader 2009] Kolda, T., and Bader, B. 2009. Tensor decompositions and applications. *SIAM Review* 51(3):455–500.
- [Lei, Wang, and Liu 2009] Lei, T.; Wang, X.; and Liu, H. 2009. Uncovering groups via heterogeneous interaction analysis. In *ICDM*, 503–512.
- [Liu et al. 2013] Liu, J.; Musialski, P.; Wonka, P.; and Ye, J. 2013. Tensor completion for estimating missing values in visual data. *TPAMI* 35(1):208–220.
- [Lu et al. 2016] Lu, C.; Tang, J.; Yan, S.; and Lin, Z. 2016. Nonconvex nonsmooth low rank minimization via iteratively reweighted nuclear norm. *TIP* 25(2):829–839.
- [Mazumder, Hastie, and Tibshirani 2010] Mazumder, R.; Hastie, T.; and Tibshirani, R. 2010. Spectral regularization algorithms for learning large incomplete matrices. *JMLR* 11:2287–2322.
- [Mu et al. 2014] Mu, C.; Huang, B.; Wright, J.; and Goldfarb, D. 2014. Square deal: Lower bounds and improved relaxations for tensor recovery. In *ICML*, 73–81.
- [Nesterov 1983] Nesterov, Y. 1983. A method for solving the convex programming problem with convergence rate  $o(1/k^2)$ . *Dokl. Akad. Nauk SSSR* 269:543–547.
- [Oseledets 2011] Oseledets, I. 2011. Tensor-train decomposition. *SIAM Journal on Scientific Computing* 33(5):2295–2317.
- [Parikh and Boyd 2013] Parikh, N., and Boyd, S. 2013. Proximal algorithms. *Foundations and Trends in Optimization* 1(3):123–231.
- [Signoretto et al. 2011] Signoretto, M.; Van de Plas, R.; De Moor, B.; and Suykens, J. 2011. Tensor versus matrix completion: a comparison with application to spectral data. *SPL* 18(7):403–406.
- [Song et al. 2017] Song, Q.; Ge, H.; Caverlee, J.; and Hu, X. 2017. Tensor completion algorithms in big data analytics. Technical report, Department of Computer Science and Engineering, Texas A&M University.
- [Tomioka and Suzuki 2013] Tomioka, R., and Suzuki, T. 2013. Convex tensor decomposition via structured Schatten norm regularization. In *NIPS*, 1331–1339.
- [Tomioka et al. 2011] Tomioka, R.; Suzuki, T.; Hayashi, K.; and Kashima, H. 2011. Statistical performance of convex tensor decomposition. In *NIPS*, 972–980.
- [Tomioka, Hayashi, and Kashima 2010] Tomioka, R.; Hayashi, K.; and Kashima, H. 2010. Estimation of low-rank tensors via convex optimization. *arXiv preprint*.
- [Xu et al. 2013] Xu, Y.; Hao, R.; Yin, W.; and Su, Z. 2013. Parallel matrix factorization for low-rank tensor completion. *IPI* 9(2):601–624.
- [Yao et al. 2017] Yao, Q.; Kwok, J.; Gao, F.; Chen, W.; and Liu, T.-Y. 2017. Efficient inexact proximal gradient algorithm for nonconvex problems. In *IJCAI*, 3308–3314.
- [Yao et al. 2018] Yao, Q.; Kwok, J.; Wang, T.; and Liu, T.-Y. 2018. Large-scale low-rank matrix learning with nonconvex regularizers. *TPAMI*.
- [Yu, Micol, and Xing 2015] Yu, Y.-L. and Xun, Z.; Micol, M.; and Xing, E. 2015. Minimizing nonconvex non-separable functions. In *AISTAT*, 1107–1115.

- [Yu 2013] Yu, Y.-L. 2013. Better approximation and faster algorithm using the proximal average. In *NIPS*, 458–466.
- [Zhang and Aeron 2017] Zhang, Z., and Aeron, S. 2017. Exact tensor completion using t-svd. *TSP* 65(6):1511–1526.
- [Zhang 2010a] Zhang, C. 2010a. Nearly unbiased variable selection under minimax concave penalty. *Annals of Statistics* 38(2):894–942.
- [Zhang 2010b] Zhang, T. 2010b. Analysis of multi-stage convex relaxation for sparse regularization. *JMLR* 11:1081–1107.
- [Zhong and Kwok 2014] Zhong, W., and Kwok, J. 2014. Gradient descent with proximal average for nonconvex and composite regularization. In *AAAI*, 2206–2212.